GERSHGORIN CIRCLES ASSOCIATED TO DOUBLE GRID SECOND ORDER CELLULAR NEURAL NETWORKS

Iolanda ALECSANDRESCU[*], Liviu GORAS[*#]
[*]*Faculty of Electronics and Telecommunications, "Gh Asachi" Technical University, Iasi, Romania*
[#]*Institute for Computer Science, Iasi, Romania*

Abstract: The stability of variable parameters double grid second order cell Cellular Neural Networks (CNN's) linearized in the central linear part of the cell characteristic is investigated by means of Gershgorin's theorem using spatial domain as well as spatial-frequency domain descriptions. It is shown that the stability margins towards the right-hand side of the complex plane are identical within both approaches and are larger than expected according to simulations. A conjecture regarding the limits of the characteristic polynomials roots is made and verified through simulations.
Key words: *Cellular Neural Networks, eigenvalues, Gershgorin circles.*

I. INTRODUCTION

Cellular Neural Networks (CNN's) [1-6] are regular arrays of identical cells identically coupled within a neighborhood radius usually equal to one or two cells. Designed for high speed signal/image processing they have been shown to exhibit interesting spatio-dynamic behaviors, among which pattern formation [7-11]. One of the architectures able to produce patterns is the two-grid coupled CNN which is a "sandwich" of second order two-port identical cells placed in the nodes of a homogeneous array and coupled by two homogeneous resistive grids [6,7]. In certain conditions such an autonomous CNN starting from non-zero initial conditions can produce Turing patterns whose specific is that even though the isolated cells are stable the whole array is unstable. The pattern emerges from the initial conditions and its final form depends on the spatial frequencies content of the initial conditions, the CNN cell structure, including the shapes of the nonlinearities, and the coupling.

II. TWO-GRID COUPLED CNN'S

In what follows we will briefly review the basic theory of two-grid coupled CNN's capable to produce Turing patterns for the particular case of piece-wise linear cells working in the linear central region [6]. A cell consists of a nonlinear active resistive two-port terminated on a capacitor at each port.

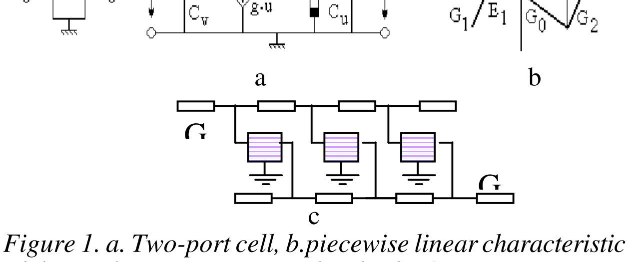

Figure 1. a. Two-port cell, b.piecewise linear characteristic of the nonlinear resistor, c. Sketch of a 1D array.

In the central linear part of the characteristic, the resistive part of the cells are described by the equations

$$\begin{aligned} i_1 &= f(u,v) = -Gu - f(u) + Gv \\ i_2 &= \tilde{g}(u,v)i_1 = (G-g)u - Gv \end{aligned} \qquad (1)$$

where R=1/G.

The analysis is greatly simplified if the nonlinearity is piecewise linear. A possible cell structure consisting of four linear elements including a voltage controlled current source and a piece-wise nonlinear resistor with port voltages denoted by u and v is represented in Fig. 1 a, b where i=f(u) is the piecewise linear characteristic of the nonlinear resistor.

The CNN based on the above cell is built by connecting the cells using two resistive grids as sketched in Fig. 1 c for the 1D case. For simplicity the discussion below will be made for 1D CNN's but generalizations to the 2D case are straightforward.

In the general case, the behavior of a 1D CNN composed of M cells is described by the following system of equations**:**

$$\begin{aligned} C_u \frac{du_i(t)}{dt} &= f(u_i, v_i) + G_u \nabla^2 u_i \\ C_v \frac{dv_i(t)}{dt} &= \tilde{g}(u_i, v_i) + G_v \nabla^2 v_i \end{aligned} \qquad i = 0, \ldots, M-1 \qquad (2)$$

where ∇^2 is the 1D Laplacean.

With some change of notations discussed in [6], the set of equations describing the CNN for the central linear part of the cell characteristics becomes

Manuscript received February 29, 2008; revised April 17, 2008

$$\frac{du_i(t)}{dt} = \gamma(f_u u_i + f_v v_i) + D_u \nabla^2 u_i \quad i = 0,...,M-1 \tag{3}$$
$$\frac{dv_i(t)}{dt} = \gamma(g_u u_i + g_v v_i) + D_v \nabla^2 v_i$$

where the relations between f_u, f_v, g_u, g_v and the circuit elements are

$$f_u = -(G+G_0),\, f_v = G,\, g_u = \frac{C_u}{C_v}(G-g),\, g_v = -\frac{C_u}{C_v}G \tag{4}$$

D_u and D_v are the diffusion coefficients and γ is a scaling coefficient. For the cell in Fig. 1.a, the above equation are valid for u-voltages within the interval [E1,E2].

III. THE DECOUPLING TECHNIQUE

In the following we analyze a 1D CNN made of piecewise nonlinear cells as shown in Fig. 1 and suppose that all voltages are within the central linear part of the cells characteristics. Using the notations from [6], we transform the system of equations by means of the change of variable

$$u_i(t) = \sum_{m=0}^{M-1} \Phi_M(i,m)\hat{u}_m(t) \quad i = 0,...,M-1 \tag{5}$$
$$v_i(t) = \sum_{m=0}^{M-1} \Phi_M(i,m)\hat{v}_m(t)$$

where $\Phi_M(i,m)$ are eigenfunctions (dependent on boundary conditions) of the 1D Laplacean.

If the set of M functions are orthogonal with respect to the scalar product in $\mathbb{C}^M$, i.e.,

$$\sum_{i=0}^{M-1} \Phi_M^*(m,i)\Phi_M(i,n) = \delta_{mn} \tag{6}$$

and can be expressed, by means of the inversion formulas

$$\hat{u}_m(t) = \sum_{i=0}^{M-1} \Phi_M^*(m,i)u_i(t) \quad m = 0,...,M-1 \tag{7}$$
$$\hat{v}_m(t) = \sum_{i=0}^{M-1} \Phi_M^*(m,i)v_i(t)$$

where

$$\Phi_M^*(m,i) = \Phi_M(i,m) \tag{8}$$

Making the change of variable and taking the scalar product of both sides of the equations, the dynamics of the 1D CNN is described by the following set of pairs of decoupled linear equations

$$\begin{bmatrix} \dot{\hat{u}}_m \\ \dot{\hat{v}}_m \end{bmatrix} = \left(\gamma \begin{bmatrix} f_u & f_v \\ g_u & g_v \end{bmatrix} - k_m^2 \begin{bmatrix} D_u & 0 \\ 0 & D_v \end{bmatrix} \right) \begin{bmatrix} \hat{u}_m \\ \hat{v}_m \end{bmatrix}, \tag{9}$$
$$m = 0, M-1$$

where k_m^2 are the eigenvalues of the 1D Laplacean, proportional to the square of sine functions [6]. For ring boundary conditions $k_m^2 = 4\sin^2\frac{m\pi}{M}$.

Thus, the set of 2×M coupled differential equations in the u and v variables transforms into M sets of pairs of second order differential equations in the new variables - the amplitudes of the spatial components of the voltages.

The natural frequencies, λ_{m1} and λ_{m2} are the roots of the characteristic polynomials

$$\lambda_m^2 + \lambda_m[k_m^2(D_u+D_v) - \gamma(f_u+g_v)] + D_u D_v k_m^4 - \tag{10}$$
$$\gamma(D_v f_u + D_u g_v)k_m^2 + (f_u g_v - f_v g_u) = 0 \;\; m = 0,...,M-1$$

The solution of the 1-D CNN equations is thus

$$u_i(t) = \sum_{m=0}^{M-1} (a_m e^{\lambda_{m1}t} + b_m e^{\lambda_{m2}t})\Phi_M(i,m) \quad i = 0,...,M-1 \tag{11}$$
$$v_i(t) = \sum_{m=0}^{M-1} (c_m e^{\lambda_{m1}t} + d_m e^{\lambda_{m2}t})\Phi_M(i,m)$$

The integration constants satisfy the constraints [8]

$$c_m = p_m a_m;\; d_m = q_m d_m \tag{12}$$

where

$$p_m = \frac{\lambda_{m1} - \gamma f_u + D_u k_m^2}{\gamma f_v};\, q_m = \frac{\lambda_{m2} - \gamma f_u + D_u k_m^2}{\gamma f_v} \tag{13}$$

and can be expressed in terms of the initial conditions of the voltages in the two "layers' of the CNN by means of the formulas

$$a_m = \frac{\hat{v}_m(0) - q_m\hat{u}_m(0)}{p_m - q_m};\; b_m = \frac{\hat{v}_m(0) - p_m\hat{u}_m(0)}{q_m - p_m} \tag{14}$$

Based on the above technique it is easy to explain the pattern formation mechanism – the existence of unstable spatial modes i.e., existence of positive values for the so-called dispersion curve and of nonzero initial values for those modes.

$$\max\left(\mathrm{Re}\;\lambda_{1,2}(k_m^2)\right) = \mathrm{Re}\;\{\gamma\frac{f_u+g_v}{2} - k_m^2\frac{D_u+D_v}{2} + \tag{15}$$
$$\sqrt{\left[\gamma\frac{(g_v-f_u)}{2} + k_m^2\frac{D_u-D_v}{2}\right]^2 + \gamma^2 f_v g_u}$$

An interesting situation is that when the origin is a stable equilibrium point for an isolated cell and an unstable equilibrium point for the whole array. The necessary conditions (Turing) that ensure the instability of an array built of stable cells linked together through resistive grids are [6]:

$$f_u + g_v < 0;\; f_u g_v - f_v g_u > 0; \tag{16}$$
$$D_v f_u + D_u g_v > 0;\; (D_v f_u - D_u g_v)^2 + 4D_u D_v f_v g_u > 0$$

The first two conditions ensure the stability of an isolated cell while the last two, the potential instability of the array. In fact, Turing-type patterns in CNN's are dependent on the following aspects: fulfillment of Turing conditions [6], dispersion curve [6], initial conditions [10], boundary conditions [11] and biasing sources signals, when they exist. It has been shown that, using a spectral decoupling technique valid for the linear part of the transient, the final pattern can be predicted to a more or less extent. The pattern formation may be regarded as a result of the competition between modes, their strengths and values being equally important. It has been also shown that the mode values and the corresponding eigenfunctions depend on the boundary conditions [7]. On the other hand, it is possible to stop the transient at a moment when none of the cells reached the nonlinear part of their characteristics. In this case the dynamics is purely linear and the array behaves as a time variable band-pass filter.

IV. NONHOMOGENEOUS CNN'S AND GERSHGORIN'S THEOREM

Basically, the decoupling mode technique was possible due to the symmetries in the set of differential equations describing an array composed of identically coupled identical cells.
On the other hand, it is obvious that any hardware realization will never rigorously fulfill such conditions to say nothing about the numerical noise which also can affect the results.
In the following we will investigate the robustness of two-grid coupled CNN's to parameter variation. The main concern will be in the existence of a band of unstable modes even though some of the cell parameters have changed. More specific, we are interested if cell parameter variations within certain limits will preserve the instability of the array. The mathematical tool which will be used is Gershgorin theorem [12,13] and an example with a CNN with 5 cells will be given. The analysis are made in the hypothesis that all parameters of the CNN except one are constant.
Gershgorin theorem gives bounds for the region in the complex plane where the eigenvalues of a matrix lie.
Given a square matrix of order n, $A = (a_{i,j}) \in \mathbb{C}$ then all its eigenvalues lie in the union of n circles:

$$\bigcup_{i=1}^{n}\left\{z \in \mathbb{C} : |z - a_{ii}| \le r_i(A)\right\} \triangleq \bigcup_{i=1}^{n}\Gamma_i(A) \triangleq \Gamma(A) \qquad (17)$$

where $r_i(A) \triangleq \sum_{j=1, j\neq i}^{n} |a_{ij}|$ (sum of off-diagonal elements in row i). $\Gamma_i(A)$ is the i-th Gershgorin circle and $\Gamma(A)$ is the Gershgorin set for A.
Noting that matrix A and its transpose A^T have the same eigenvalues, applying the above theorem for A^T yields another set $\hat{\Gamma}(A)$.
The eigenvalues of matrix A are lying in the complex plane within the intersection of the Gershgorin sets $\Gamma(A)$ and $\hat{\Gamma}(A)$.
To simplify the notations, in the following we consider as an example a 5-cell CNN with ring boundary conditions which is described by the set of state equations of order 10 (each cell is second order):

$$\begin{bmatrix}\dot{u}_0\\ \dot{u}_1\\ \dot{u}_2\\ \dot{u}_3\\ \dot{u}_4\\ \dot{v}_0\\ \dot{v}_1\\ \dot{v}_2\\ \dot{v}_3\\ \dot{v}_4\end{bmatrix} = \begin{bmatrix}\gamma f_u-2D_u & D_u & 0 & 0 & D_u & \gamma f_v & 0 & 0 & 0 & 0\\ D_u & \gamma f_u-2D_u & D_u & 0 & 0 & 0 & \gamma f_v & 0 & 0 & 0\\ 0 & D_u & \gamma f_u-2D_u & D_u & 0 & 0 & 0 & \gamma f_v & 0 & 0\\ 0 & 0 & D_u & \gamma f_u-2D_u & D_u & 0 & 0 & 0 & \gamma f_v & 0\\ D_u & 0 & 0 & D_u & \gamma f_u-D_u & 0 & 0 & 0 & 0 & \gamma f_v\\ \gamma g_u & 0 & 0 & 0 & 0 & \gamma g_v-D_v & D_v & 0 & 0 & 0\\ 0 & \gamma g_u & 0 & 0 & 0 & D_v & \gamma g_v-2D_v & D_v & 0 & 0\\ 0 & 0 & \gamma g_u & 0 & 0 & 0 & D_v & \gamma g_v-2D_v & D_v & 0\\ 0 & 0 & 0 & \gamma g_u & 0 & 0 & 0 & D_v & \gamma g_v-2D_v & D_v\\ 0 & 0 & 0 & 0 & \gamma g_u & D_v & 0 & 0 & D_v & \gamma g_v-2D_v\end{bmatrix} \cdot \begin{bmatrix}u_0\\ u_1\\ u_2\\ u_3\\ u_4\\ v_0\\ v_1\\ v_2\\ v_3\\ v_4\end{bmatrix}$$

In the next section we will present a case study with a CNN with the above dimension, i.e., with 5 cells.
Using the change of variable discussed above, the equations decouple and become

$$\begin{bmatrix}\dot{\hat{u}}_0\\ \dot{\hat{v}}_0\\ \dot{\hat{u}}_1\\ \dot{\hat{v}}_1\\ \dot{\hat{u}}_2\\ \dot{\hat{v}}_2\\ \dot{\hat{u}}_3\\ \dot{\hat{v}}_3\\ \dot{\hat{u}}_4\\ \dot{\hat{v}}_4\end{bmatrix} = \begin{bmatrix}\gamma f_u-k_0^2D_u & \gamma f_v & 0 & 0 & 0 & 0 & 0 & 0 & 0 & 0\\ \gamma g_u & \gamma g_v-k_0^2D_v & 0 & 0 & 0 & 0 & 0 & 0 & 0 & 0\\ 0 & 0 & \gamma f_u-k_1^2D_u & \gamma f_v & 0 & 0 & 0 & 0 & 0 & 0\\ 0 & 0 & \gamma g_u & \gamma g_v-k_1^2D_v & 0 & 0 & 0 & 0 & 0 & 0\\ 0 & 0 & 0 & 0 & \gamma f_u-k_2^2D_u & \gamma f_v & 0 & 0 & 0 & 0\\ 0 & 0 & 0 & 0 & \gamma g_u & \gamma g_v-k_2^2D_v & 0 & 0 & 0 & 0\\ 0 & 0 & 0 & 0 & 0 & 0 & \gamma f_u-k_3^2D_u & \gamma f_v & 0 & 0\\ 0 & 0 & 0 & 0 & 0 & 0 & \gamma g_u & \gamma g_v-k_3^2D_v & 0 & 0\\ 0 & 0 & 0 & 0 & 0 & 0 & 0 & 0 & \gamma f_u-k_4^2D_u & \gamma f_v\\ 0 & 0 & 0 & 0 & 0 & 0 & 0 & 0 & \gamma g_u & \gamma g_v-k_4^2D_v\end{bmatrix} \cdot \begin{bmatrix}\hat{u}_0\\ \hat{v}_0\\ \hat{u}_1\\ \hat{v}_1\\ \hat{u}_2\\ \hat{v}_2\\ \hat{u}_3\\ \hat{v}_3\\ \hat{u}_4\\ \hat{v}_4\end{bmatrix}$$

where the new variables are the spectra of the old ones with respect to the set of orthogonal spatial functions corresponding to the Discrete Fourier Series of order M.
For each of the two matrices that describe de dynamics of the array two Gershgorin sets can be determined. The fundamental difference between the two approaches is that the latter implies the homogeneity of the whole array. It can be thus used only for homogeneous variations of the parameters. It is interesting to compare the results of the two approaches in what concerns the rightmost circle whose position is related to the existence of a band of unstable modes. It is also worth mentioning that, due to the symmetries of the array and thus of the equations, there are only two values for the Gershgorin circles for each CNN, only the radii being variable. As far as γ, f_u, g_v, D_u and D_v are constant, the centers of the circles are constant as well, only the radii being variable. Thus, the centers of the Gershgorin circles for the first matrix are at the points

$c_1 = \gamma f_u - 2D_u$; $c_2 = \gamma g_v - 2D_v$

and the respective radii are:

$r_1 = |2D_u| + |\gamma g_u|$; $r_2 = |2D_v| + |\gamma f_v|$ (computed for columns) and

$r_1 = |2D_u| + |\gamma f_v|$; $r_2 = |2D_v| + |\gamma g_u|$ (computed for rows).

The centers of the Gershgorin circles determined from the matrix of the decoupled equation are

$c_1 = \gamma f_u - k_m^2 D_u$; $c_2 = \gamma g_v - k_m^2 D_v$ and the radii are $r_1 = |\gamma f_v|$; $r_2 = |\gamma g_u|$ for both centers. It can be observed that for k_m^2=0 and D_u and D_v positive, two of the maximum abscissa computed with the two methods coincide i.e.,

$x_{1\max} = \gamma f_u + |\gamma g_u|$; $x_{2\max} = \gamma g_v + |\gamma f_v|$.

The results are coherent with the family of dispersion curves with variable f_u shown in Fig. 2

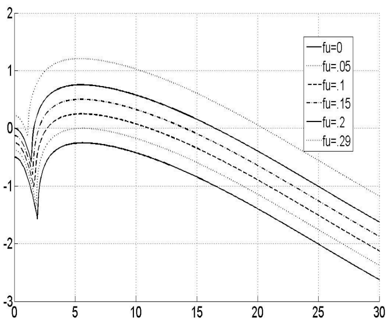

Figure.2. Family of dispersion curves for variable f_u.

V. A CASE STUDY

Consider a 1D CNN with M=10. We choose the following values which satisfy Turing conditions (16):

$$f_u = 0.1,\ f_v = -1.2,\ g_u = 0.1,$$

$$g_v = -0.2,\ D_u = 1,\ D_v = 150,\ \gamma = 5$$

The peak of the dispersion curve is located at the value [6]:

$$k_p^2 = \left[(g_v - f_u) + \frac{(D_u + D_v)}{\sqrt{D_u D_v}} \sqrt{-f_v g_u} \right] \frac{\gamma}{D_v - D_u} \tag{18}$$

In our case, $k_p^2 = 0.1333$ and $\operatorname{Re}\lambda(k_p^2) = 0.2253$.

Gershgorin circles have centers located at the abscissas :

$c_1 = \gamma f_u - 2D_u = -1.5;\ c_2 = \gamma g_v - 2D_v = -301$

The radii computed for columns and rows are

$r_1 = |2D_u| + |\gamma g_u| = 2.5; r_2 = |2D_v| + |\gamma f_v| = 306$ and

$r_1 = |2D_u| + |\gamma f_v| = 8;\ r_2 = |2D_v| + |\gamma g_u| = 300.5$

respectively.

As expected, the radii do not depend on f_u.

Thus, the rightmost abscissa for the eigenvalues is *min*{8-1.5, 300.6-301}=5. However, this limit is larger than the greatest real part of the eigenvalues so that there is no reason to state that the array will be unstable. A sketch of the four Gershgorin circles for columns and rows corresponding to the numerical example is presented in Fig. 3.

Using the matrix for decoupled equations the Gershgorin centers and radii for the adopted values of the parameters are given by the core matrix

$$\begin{bmatrix} 0.5 - k_m^2 & -6 \\ 0.5 & -1 - 150k_m^2 \end{bmatrix}$$

Where $k_m^2 \in [0, 4]$.

Thus, the abscissas of centers of the Gershgorin circles are 0.5-k_m^2 i.e. they have values between -3.5 and 0.5 and between -601 and -1 with radii 0.5 and 6. The rightmost abscissa of the circles is 5 as in the previous case.

When f_u varies some of the above values change.

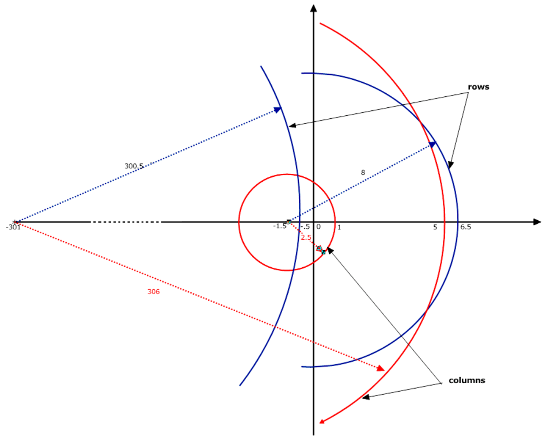

Figure.3. Sketch of the four Gershgorin circles for columns and rows corresponding to the numerical example

The Gershgorin circles for the same example for decoupled modes matrix are given in Fig. 4 for rows and Fig. 5 for columns where asterisks represent the centers of the circles.

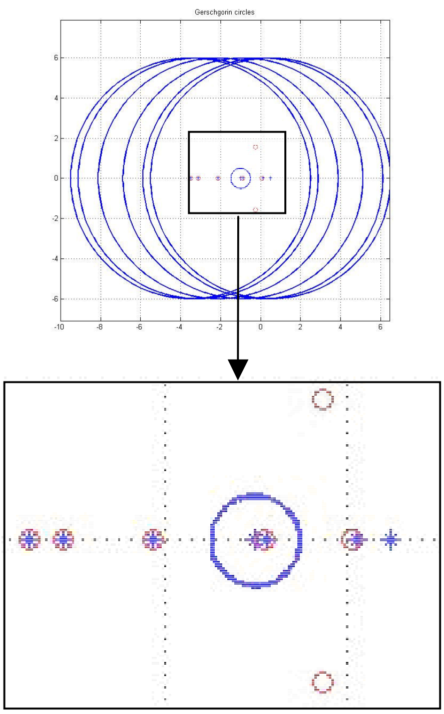

Figure.4.Rows Gershgorin circles for the decoupled modes matrix

Again, when f_u varies some of the above values change.

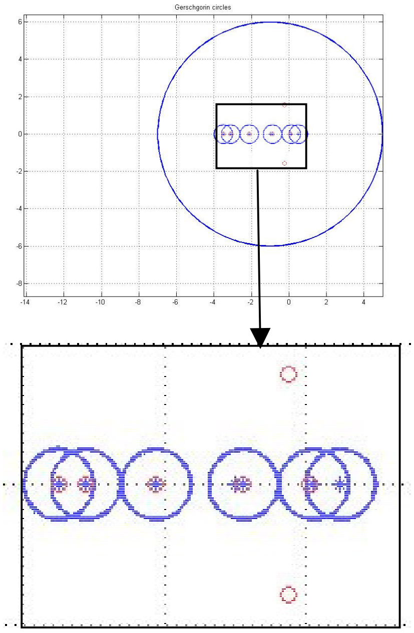

Figure 5.Columns Gershgorin circles for the decoupled modes matrix

From the above figures it can be seen that many of the circles have no influence on the stability limits.
In the following we present several results when other parameters vary, i.e., γ, D_v, f_v .and D_u. In the table below the Gershgorin circles and the eigenvalues for each casa have been represented. Since the eigenvalues have been represented with only four decimals, some of them, which are very close, appear to be equal.

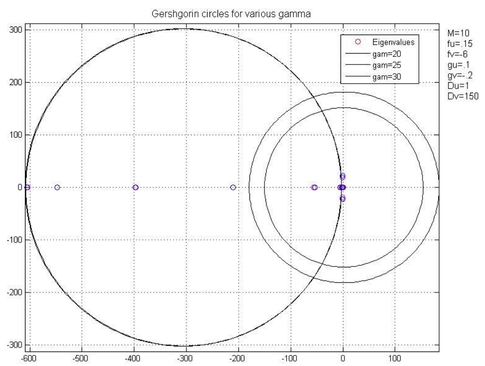

γ=20	-603.6017 -546.2653 -546.2653 -396.0998 -396.0998 -210.1616 -210.1616 -57.2887 -57.2887 -1.3983 -1.3882 -1.3882 -1.0579 -1.0579 -0.5000 -0.5000 -0.2234 -0.2234 0.4848 0.4848
γ=25	-604.3793 -547.0197 -547.0197 -396.7626 -396.7626 -210.5335 -210.5335 -55.9758 -55.9758 -2.9511 -2.9511 -0.8707 -0.6250 -0.6250 -0.5534 -0.5534 0.1895 0.1895 0.6067 0.6067
γ=30	-605.1083 -547.7208 -547.7208 -397.3525 -397.3525 -210.7702 -210.7702 -54.0041 -54.0041 -5.1727 -5.1727 -0.7500 -0.7500 -0.3917 -0.1024 -0.1024 0.5294 0.5294 0.5934 0.5934

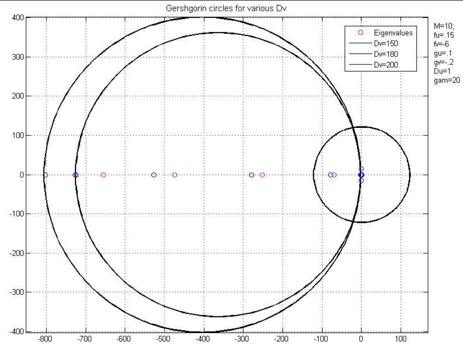

D_v =150	-603.6017 -546.2653 -546.2653 -396.0998 -396.0998 -210.1616 -210.1616 -57.2887 -57.2887 -1.3983 -1.3882 -1.3882 -1.0579 -1.0579 -0.5000 -0.5000 -0.2234 -0.2234 0.4848 0.4848
D_v =180	-723.6679 -654.8793 -654.8793 -474.7410 -474.7410 -251.8069 -251.8069 -69.4224 -69.4224 -1.3321 -0.9849 -0.9849 -0.7134 -0.7134 -0.5000 -0.5000 -0.1232 -0.1232 0.6710 0.6710
D_v =200	-803.7010 -727.2765 -727.2765 -527.1519 -527.1519 -279.5396 -279.5396 -77.3936 -77.3936 -1.2990 -0.9483 -0.9483 -0.5000 -0.5000 -0.3815 -0.3815 -0.0730 -0.0730 0.7644 0.7644

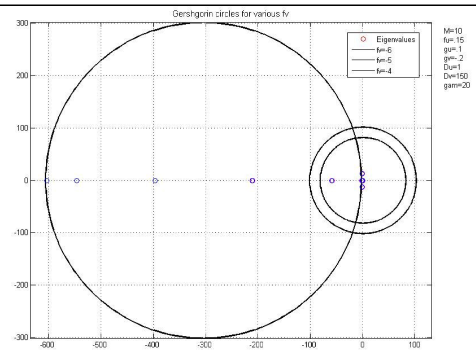

f_v =-6	-603.6017 -546.2653 -546.2653 -396.0998 -396.0998 -210.1616 -210.1616 -57.2887 -57.2887 -1.3983 -1.3882 -1.3882 -1.0579 -1.0579 -0.5000 -0.5000 -0.2234 -0.2234 0.4848 0.4848
f_v =-5	-603.6681 -546.3386 -546.3386 -396.2008 -396.2008 -210.3514 -210.3514 -57.9953 -57.9953 -1.3319 -0.9845 -0.9845 -0.6816 -0.6816 -0.5000 -0.5000 -0.1223 -0.1223 0.6745 0.6745
f_v =-4	-603.7345 -546.4119 -546.4119 -396.3018 -396.3018 -210.5407 -210.5407 -58.6849 -58.6849 -1.2655 -0.9112 -0.9112 -0.5000 -0.5000 -0.0214 -0.0214 0.0080 0.0080

	0.8639 0.8639
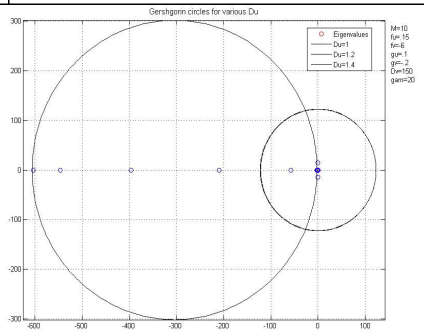	
D_u=1	-603.6017 -546.2653 -546.2653 -396.0998 -396.0998 -210.1616 -210.1616 -57.2887 -57.2887 -1.3983 -1.3882 -1.3882 -1.0579 -1.0579 -0.5000 -0.5000 -0.2234 -0.2234 0.4848 0.4848
D_u=1.2	-603.6012 -546.2647 -546.2647 -396.0990 -396.0990 -210.1602 -210.1602 -57.2832 -57.2832 -2.1988 -1.7821 -1.7821 -1.4701 -1.4701 -0.7478 -0.7478 -0.5000 -0.5000 0.2069 0.2069
D_u=1.4	-603.6007 -546.2641 -546.2641 -396.0982 -396.0982 -210.1587 -210.1587 -57.2777 -57.2777 -2.9993 -2.5063 -2.5063 -1.5520 -1.5520 -1.2722 -1.2722 -0.5000 -0.5000 -0.0710 -0.0710

From the above results it can be seen again that the Gershgorin circles give larger limits for the eigenvalues so that their use should be considered with care. On the other hand, using the dispersion curves for homogeneous variations of the parameters, it is easy to determine if the network is stable or not. It is likely that, if for homogeneous variations for f_u, i.e., $f_u-\delta$ and $f_u+\delta$ the network is unstable, for random variation of f_u with the same magnitude, the network should remain unstable as well. To verify the above, the frequency response of the CNN's having nonzero initial condition the u-voltage on a single cell, after several time steps (same for all simulations) have been studied. The FFT of the spatial signal frozen at a moment when no cell reached the nonlinearity has been recorded for the following four types of situations i.e., homogeneous nominal f_u, homogeneous $f_u-\delta$, homogeneous $f_u+\delta$, nonhomogeneous f_u random with values from the 2 element set { $f_u-\delta, f_u+\delta$ } and nonhomogeneous random from the infinite set [$f_u-\delta, f_u+\delta$].

The simulations showed that in all cases the frequency response for nonhomogeneous situations was placed between that for $f_u-\delta$ and $f_u+\delta$ no matter what was the value of δ (chosen such that for $f_u-\delta$ the CNN was unstable). The simulations were made for δ equal to 0%, 1%, 5% and 10% of f_u.

These results show again that most probably the Gershgorin circles give much larger limits for the eigenvalues than those corresponding to the situation described above. The peaks of the frequency response for homogeneous variation of f_u are given in the following table. The simulation results are given in Fig. 6

	f_u-δ	f_u+δ
δ=1%f_u	~1	~1.4
δ=5%f_u	~0.52	~2.5
δ=10%f_u	~0.5	~5.5

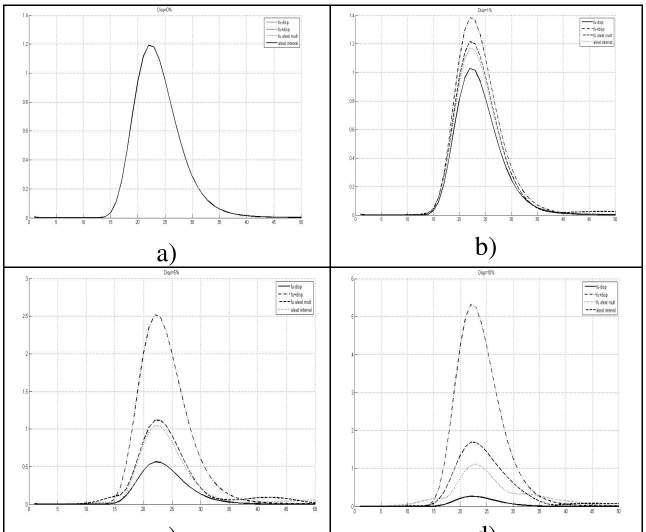

a) b) c) d)

Figure 6. Frequency response for constant f_u, (a), $f_u+\delta$, $f_u-\delta$, f_u random from { $f_u-\delta, f_u+\delta$ } and f_u random from [$f_u-\delta, f_u+\delta$] for δ =1% f_u (b) δ =5% f_u (c) and δ =10% f_u (d)

Changing the seeds for randomizing the f_u parameters for the situations where they are randomly chosen either from the 2 element set { $f_u-\delta, f_u+\delta$ } or from the infinite set [$f_u-\delta, f_u+\delta$] the results were again placed between the two limits corresponding to $f_u-\delta$ and $f_u+\delta$. The peaks are presented in the table and the frequency response at the same moment for all situations in Fig. 7

	Peak for f_u randomly chosen from {f_u–δ, f_u+δ}	Peak for f_u randomly chosen from [f_u–δ, f_u+δ]
δ=1%f_u	between 1.1 and 1.2	betwee 1.1 and 1.25
δ=5%f_u	between 1.15 and 1.6	between 0.9 and 1.5
δ=10%f_u	between 1 and 2.55	between 1.1 and 1.9

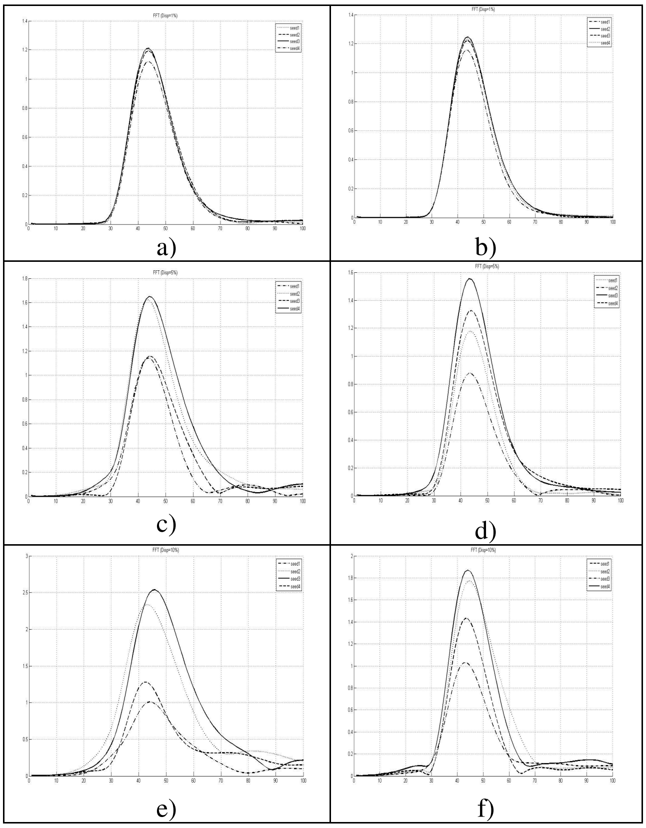

Figure 7. Frequency response of the CNN for δ =1% f_u , δ =5% f_u and δ =10% f_u with random parameters from the set { $f_u - \delta$, $f_u + \delta$ } (a,c,e) and random from the infinite set [$f_u - \delta$, $f_u + \delta$] (b,d,f) for four seeds.

VI. CONCLUDING REMARKS

The investigation of double grid second order cell CNN stability for variable parameters linearized in the central linear part of the cell characteristic using Gershgorin's theorem is rather simple due to the symmetries and sparsity of the state matrix. The rightmost limit of the Gershgorin domains obtained using the initial state matrix and the matrix of the decoupled modes are identical and are larger than expected according to simulations. Intensive simulations seem to confirm that if a CNN is unstable for $f_u - \delta$ random variation of f_u with dispersion δ correspond to an unstable CNN as well with the spatial frequency peaks placed above that for homogeneous CNN with $f_u - \delta$ and below that for homogeneous CNN with $f_u + \delta$.

REFERENCES

[1] L. O. Chua, L. Yang, "Cellular Neural Networks: Theory", IEEE Trans. Circuits Syst., vol. 35, no 10, pp. 1257-1272, October 1988.
[2] L. O. Chua, L. Yang, "Cellular Neural; Networks: Applications", IEEE Trans. Circuits Syst., vol. 35, no 10, pp 1273-1290, October 1988.
[3] K. R. Crounse, L. O. Chua, "Methods for image processing and pattern formation in Cellular Neural Networks: A Tutorial", ", IEEE Trans. Circuits Syst, vol.42, no. 10, pp. 583-601, October 1995.
[4] B. E. Shi, "Gabor-type filtering in space and time with cellular neural networks", IEEE Trans.on Circuits and Syst., Vol. 45, No. 2, February 1998.
[5] L. Goras, L. O. Chua, D. M. W. Leenaerts, "Turing Patterns in CNN's-Part I: Once Over Lightly", IEEE Trans. Circuits Syst, vol.42, pp. 602-611, October 1995.
[6] L. Goraş, L. O. Chua, "Turing Patterns in CNN's - Part II: Equations and Behaviors", IEEE Trans. Circuits Syst, vol.42, pp. 612-626, October 1995.
[7] L. Goraş, "On Pattern Formation in Cellular Neural Networks", NATO Advanced Research Workshop, Siena, Italy, 22-24 October, 2002; published in V. Piuri , M. Gori , S. Ablameyko and L. Goras, (editors) "Limitations and Future Trends in Neural Computation", Volume 186 NATO Science Series: Computer & Systems Sciences;
[8] L. Goraş, L. O. Chua, Turing Patterns in CNN's Based on a New Cell, Proc. of the Fourth International Workshop on Cellular, Neural Networks and Their Applications, CNNA'96, pp.103-108, Seville, Spain, June 1996.
[9] T. Teodorescu, L. Goraş, "On the Dynamics of Turing Pattern Formation in 1D CNN's", Proc. SCS'97, Iasi, pp. 109-112, October 1997.
[10] L. Goraş, L. O. Chua, "On the Role of CNN Initial Conditions in Turing Pattern Formation", Proc. SCS'97, pp 105-108
[11] L. Goraş, L. O. Chua, "On the Influence of CNN Boundary Conditions in Turing Pattern Formation", Proc. ECCTD'97, Budapest, pp. 383-388, 1997
[12] L. Cvetkovic, V. Kostic, R. Varga, " A new Gershgorin-type eigenvalues inclusion set", Electronic Transactions on Numerical Analysis, vol. 18, pp73-80, 2004
[13] Yogesh V. Hote D. Roy Choudhury J.R.P. Gupta "Gerschgorin Theorem and its Applications in Control System Problems", Industrial Technology, ICIT 2006, IEEE International Conference on, 2006